Stem Cell Reports, Volume *18*

Supplemental Information

A human *in vitro* neuronal model for studying homeostatic plasticity at the network level

Xiuming Yuan, Sofía Puvogel, Jon-Ruben van Rhijn, Ummi Ciptasari, Anna Esteve-Codina, Mandy Meijer, Simon Rouschop, Eline J.H. van Hugte, Astrid Oudakker, Chantal Schoenmaker, Monica Frega, Dirk Schubert, Barbara Franke, and Nael Nadif Kasri

Supplemental information

Supplemental information includes the five supplemental figures, supplemental discussion, four supplemental tables, supplemental experimental procedures, and supplemental references.

Supplemental items

Supplemental Figure S1. Quantification of microelectrode array (MEA) parameters in Ctrl2 and Ctrl3 neurons. Related to Figure 1.
Supplemental Figure S2. Effect of 1-naphthyl acetyl spermine trihydrochloride (NASPM) treatment on the neuronal network activity. Related to Figure 2.
Supplemental Figure S3. Miniature excitatory postsynaptic current (mEPSC) activity in Ctrl 3 neurons. Related to Figure 3.
Supplemental Figure S4. Gene expression changes in tetrodotoxin (TTX)-treated neurons. Related to Figure 4.
Supplemental Figure S5. Astrocytes and neurons share some transcriptional changes in response to TTX-induced neuronal activity suppression. Related to Figure 5.

Supplemental tables (Table S1-3 were added as separate excel files)

Table S1: Tab 1, Results from differential expression analysis for human induced pluripotent stem cell (hiPSC)-derived neurons treated with TTX for 48 h, related to Figure 4. Tab 2, Results from gene ontology (GO) enrichment analysis for hiPSC-derived neurons treated with TTX for 48 h, related to Figure 4. Tab 3 and 4, Results from comparison between differentially expressed genes (DEGs) in hiPSC-derived neurons induced by TTX treatment and genes related to neurodevelopmental disorders (NDDs) as well as confident autism-related genes, related to Figure 4. Tab 5, Results from SYNGO analysis for human induced pluripotent stem cell (hiPSC)-derived neurons treated with TTX for 48 h, related to Figure 4.

Table S2: Tab 1, Results from differential expression analysis for rat astrocytes treated with TTX for 48 h, related to Figure 5. Tab 2, Results from GO enrichment analysis for rat astrocytes treated with TTX for 48 h, related to Figure 5. Tab 3 and 4, Results from comparison between DEGs in rat astrocytes induced by TTX treatment and genes related to NDDs as well as confident autism-related genes, related to Figure 5. Tab 5, Results from SYNGO analysis for rat astrocytes treated with TTX for 48 h, related to Figure 5.

Table S3: Statistics per figure, including all means, SEM and test statistics.

Table S4: List of quantitative polymerase chain reaction (q-PCR) primers used in this study (added in this manuscript), related to Figure 5.

Supplemental experimental procedures

Supplemental items

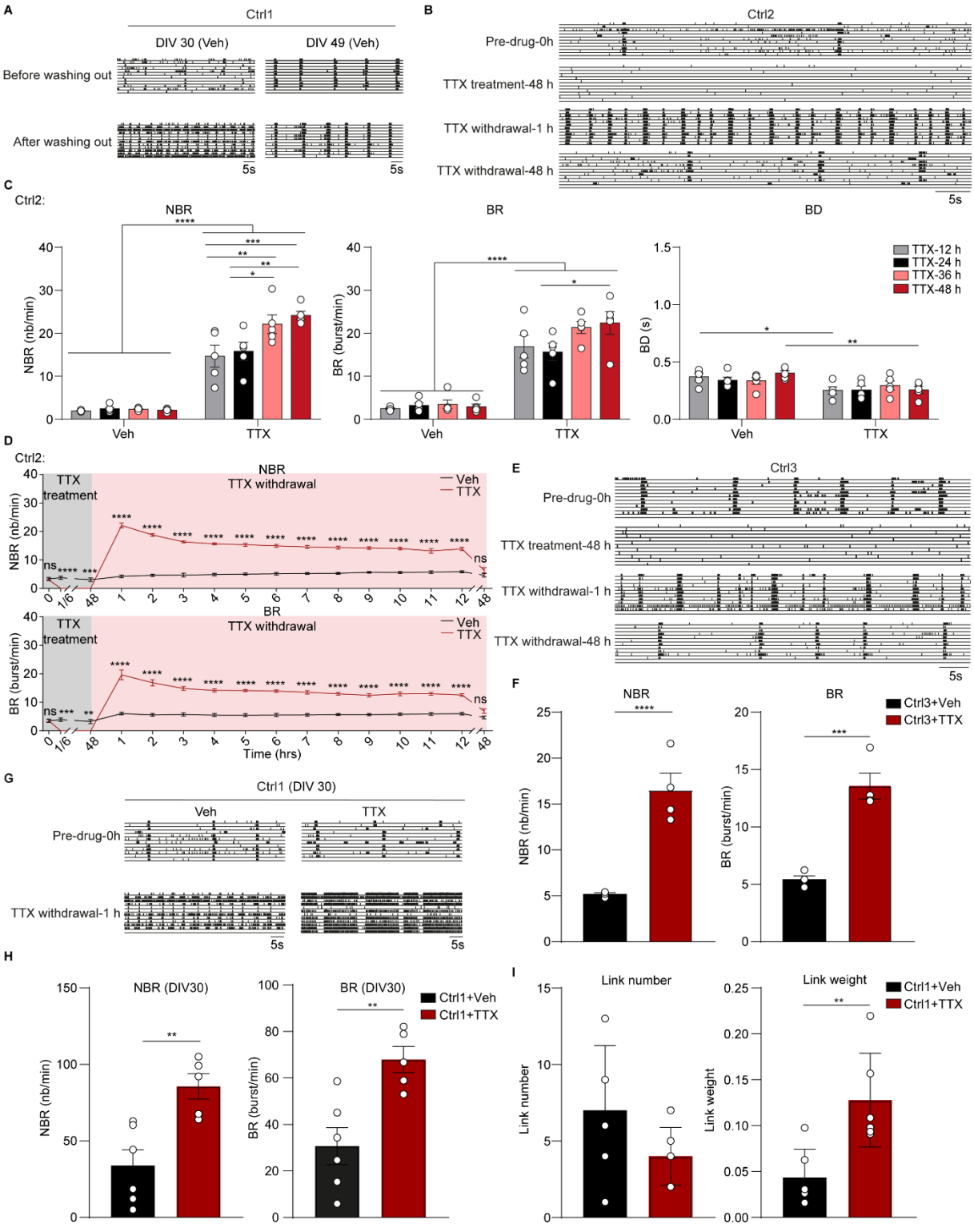

Supplemental Figure S1. Quantification of microelectrode arrays (MEAs) parameters in Ctrl2 and Ctrl3 neurons. Related to Figure 1.(A) Representative raster plots showing 1 min of spontaneous activity from hiPSC-derived neuronal networks (Ctrl1) before and after washing out procedure at days *in vitro* (DIV) 30 and DIV 49. (B) Representative raster plots showing 1 min of spontaneous activity from hiPSC-derived neuronal networks (Ctrl2) before and after TTX treatment, including before addition of TTX (Pre-drug-0 h), 48 h after addition of TTX (TTX treatment-48 h), 1 h after TTX withdrawal (TTX withdrawal-1 h), and 48 h after TTX withdrawal (TTX withdrawal-48 h). (C) Bar graphs showing the effect

of 12 h, 24 h, 36 h, and 48 h TTX treatment on the mean network burst rate (NBR), mean burst rate (BR), and mean burst duration (BD) for Ctrl2 neuronal networks. All MEA parameters were measured 1 h after TTX withdrawal. n = number of MEA wells/batches: Veh n = 5/1 for each group, TTX n = 5/1 for each group. (D) Quantification of NBR and BR over time for vehicle-treated (Veh) and 48 h TTX-treated (TTX) neurons (Ctrl2). n = number of MEA wells/batches: Veh n = 8/2, TTX n = 10/2. (E) Representative raster plots showing 1 min of spontaneous activity from hiPSC-derived neuronal networks (Ctrl3) before and after TTX treatment, including before addition of TTX (Pre-drug-0 h), 48 h after addition of TTX (TTX treatment-48 h), 1 h after TTX withdrawal (TTX withdrawal-1 h), and 48 h after TTX withdrawal (TTX withdrawal-48 h). (F) Bar graphs showing the quantification of NBR and BR for (E) at TTX withdrawal-1 h. n = number of MEA wells/batches: Veh n = 4/1, TTX n = 4/1. (G) Representative raster plots showing 1 min of spontaneous activity from hiPSC-derived neuronal networks (Ctrl1) before and after TTX treatment at DIV 30, including before addition of TTX (Pre-drug-0h) and 1 h after TTX withdrawal (TTX withdrawal-1 h). (H) Bar graphs showing the quantification of NBR and BR for (G) at TTX withdrawal-1 h. n = number of MEA wells/batches: Veh n = 6/1, TTX n = 5/1. (I) Comparison of the number of links and weight of links between vehicle-treated (Veh) and TTX-treated (TTX) conditions in Ctrl1 neuronal networks. n = number of MEA wells/batches: Veh n = 6/1, TTX n = 6/1. Data represent means ± SEM. ns: not significant, *$P < 0.05$, **$P < 0.005$, ***$P < 0.0005$, ****$P < 0.0001$. For panel C and D, two-way ANOVA test followed by a *post-hoc* Bonferroni correction was performed between conditions. For panel F and H, unpaired Student's T-test was performed between two groups. For panel I, Mann Whitney U test with Bonferroni correction for multiple testing was performed between conditions. All means, SEM and test statistics are listed in Table S3.

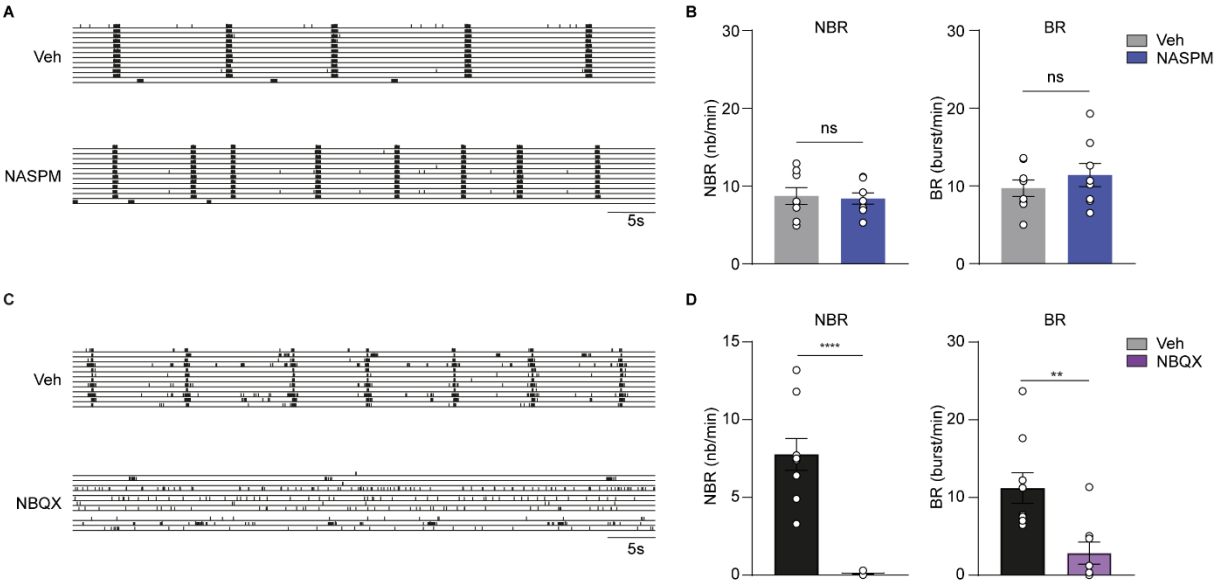

Supplemental Figure S2. Effect of 1-naphthyl acetyl spermine trihydrochloride (NASPM) treatment on the neuronal network activity. Related to Figure 2. (A) Representative raster plots showing 1 min of spontaneous activity from Ctrl1 neuronal networks grown on MEAs at DIV 49. Where indicated, the cells were vehicle-treated (Veh), or cells were treated with 10 µM NASPM before TTX application (NASPM). (B) Bar graphs showing the quantification of NBR and BR for (A). n = number of MEA wells/batches: Veh n = 8/2, NASPM n = 8/2. (C) Representative raster plots showing 1 min of spontaneous activity from Ctrl1 neuronal networks grown on MEAs at DIV 49. Where indicated, the cells were vehicle-treated (Veh), or cells were treated with 50 µM NBQX (NBQX). (D) Bar graphs showing the quantification of NBR and BR for (C). n = number of MEA wells/batches: Veh n = 9/1, NBQX n = 8/1. Data represent means ± SEM. ns: not significant, $^{**}P < 0.005$, $^{****}P < 0.0001$. For panel B and D, unpaired Student's T-test was performed between two groups. All means, SEM and test statistics are listed in Table S3.

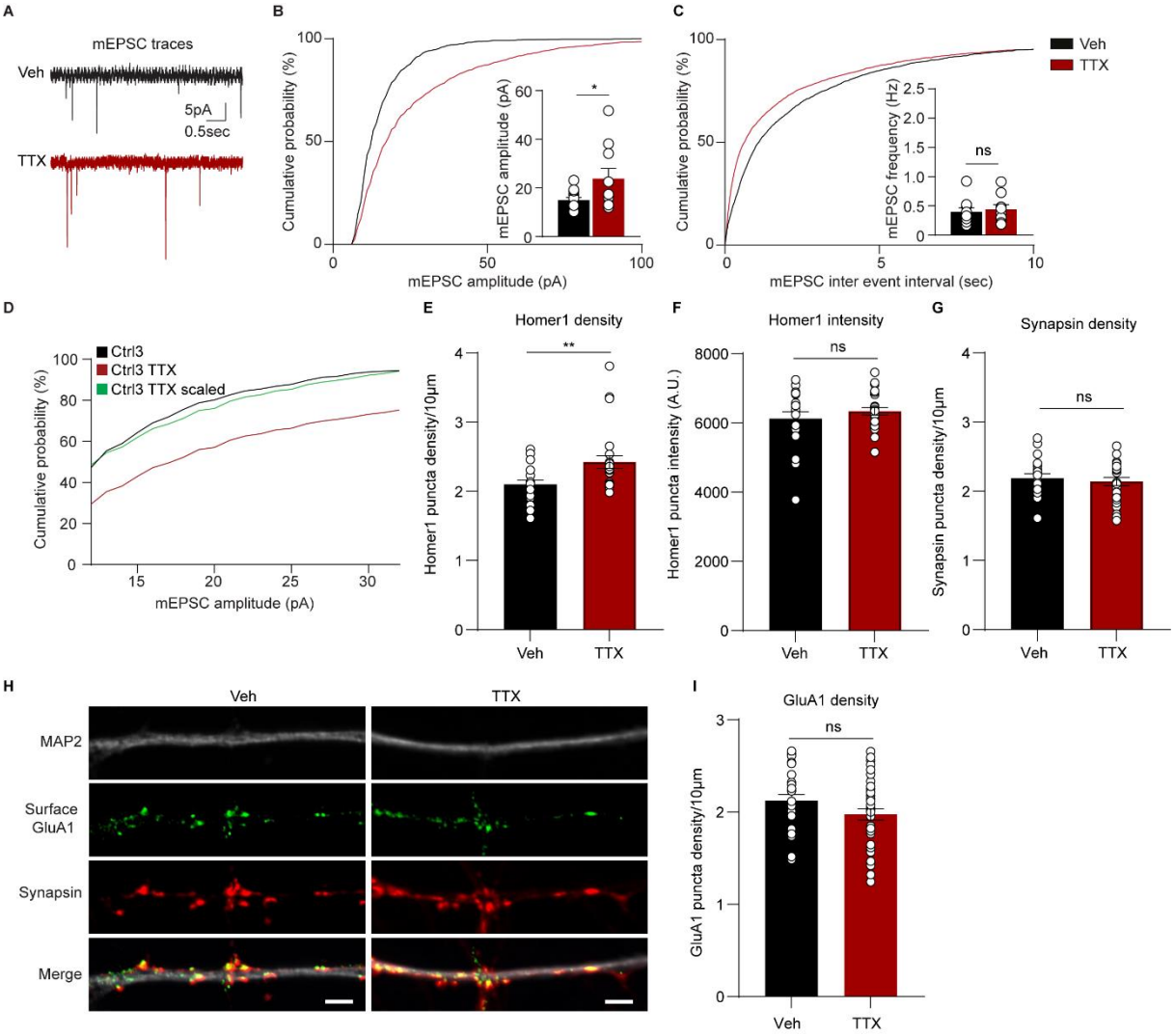

Supplemental Figure S3: Miniature excitatory postsynaptic current (mEPSC) activity in Ctrl 3 neurons. Related to Figure 3. (A) Representative mEPSC traces of vehicle-treated (Veh) and 48 h-TTX treated (TTX) neurons (Ctrl3). (B-D) Quantification of the amplitude (B) and frequency of mEPSCs (C) in Veh and TTX conditions. n = number of cells/batches: Veh n = 11/3, TTX n = 10/3. Rescaled cumulative mEPSC amplitude (Scaling = TTX values * 1.19) (D). (E-G) Quantification of Homer1 puncta (number per 10 µm), Homer1 puncta intensity (A.U., averaged corrected integrated density per unit), and Synapsin1/2 puncta (number per 10 µm). n = number of cells/batches: Veh n = 20/1, TTX n = 25/1. (H) Representative images of vehicle-treated (Veh) and 48 h TTX-treated (TTX) neurons (Ctrl1) stained for MAP2 (grey), GluA1 (green), and synapsin 1/2 (red) (scale bar 5 µm). (I) Quantification of Synapsin/GluA1 co-localized puncta (number per 10 µm). n = number of cells/batches: Veh n = 25/1, TTX n = 37/1. Data represent means ± SEM. ns: not significant, *P < 0.05, **P < 0.005, unpaired Student's T-test was performed between two groups. All means, SEM and test statistics are listed in Table S3.

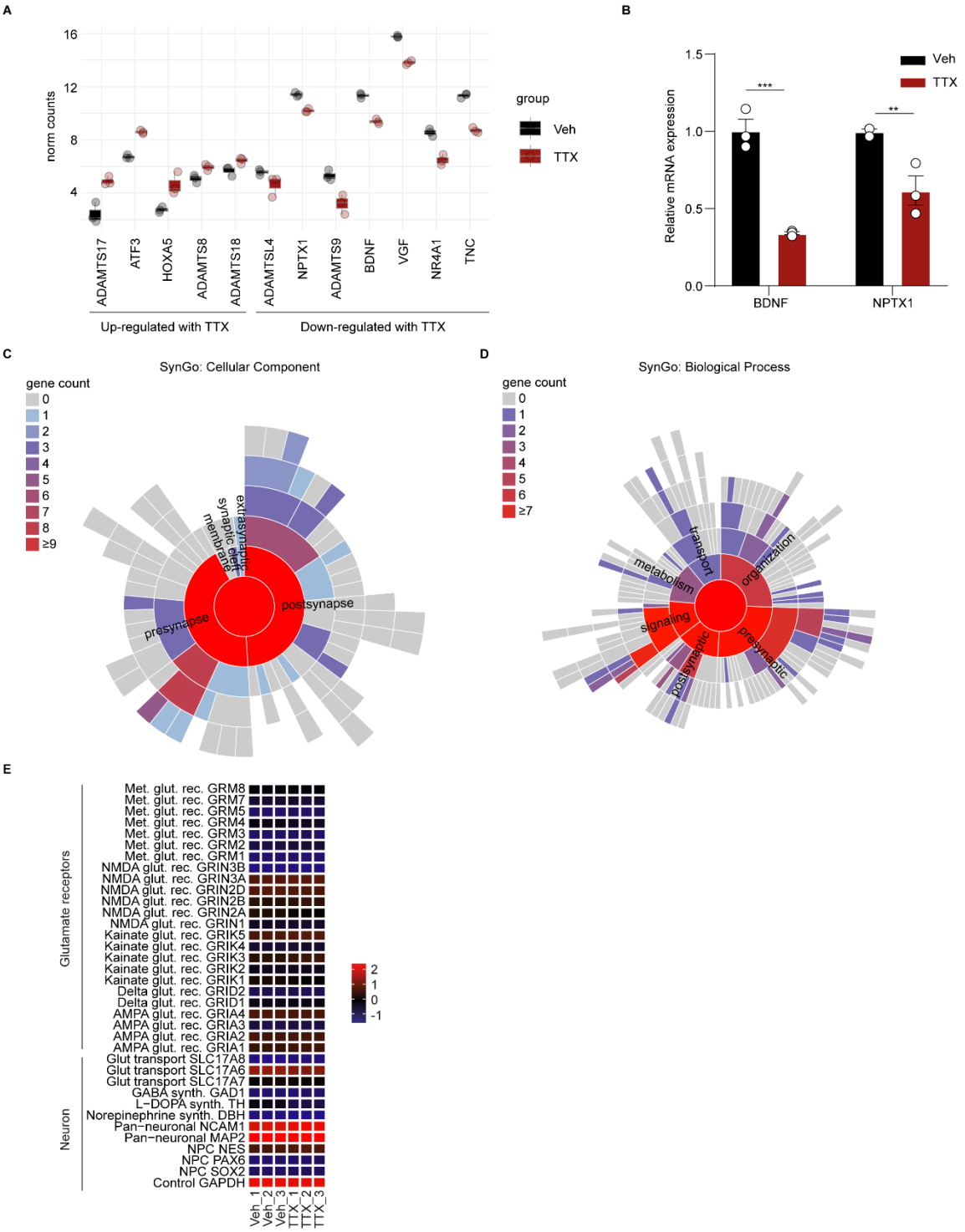

Supplemental Figure S4. Gene expression changes in TTX-treated neurons. Related to Figure 4. (A) Boxplot depicting the expression of selected DEGs (DESeq2 normalized counts), in both TTX- (red) and vehicle-treated neurons (black). (B) Bar graph showing relative messenger RNA (mRNA) expression of selected genes in TTX treated neurons (TTX-treated neurons = red, and vehicle-treated neurons = black). n = 3 replicates for each group. Data represent means ± SEM. **P < 0.005, ***P < 0.0005, two-way ANOVA test followed by a *post-hoc* Bonferroni correction was performed between conditions. All means, SEM and test statistics are listed in Table S3. (C-D) Sunburst plots for synaptic GO analysis of DEGs in response to TTX treatment in hiPSC-derived neurons (Ctrl1, absolute

log_2 fold change (Log_2FC) > 0.58 and adjusted P value < 0.05), including Cellular Component (C) and Biological Process (D). 41 DEGs have a Cellular Component annotation, 30 DEGs for Biological Processes (a gene may have multiple annotations). 0 Cellular Component terms are significantly enriched at 1% FDR (testing terms with at least three matching input genes), 0 for Biological Processes. Enrichment analyses were performed using 1-sided Fisher exact tests (with “greater than” for the alternative hypothesis) and the False Discovery Rate (FDR) method was applied for multiple testing correction. Synaptic GO analysis was performed with the SynGo (Koopmans et al., 2019). Warmer colors represent the predominance of genes associated with the respective pathway. (E) Heatmap depicting scaled expression of glutamate receptors and neuronal marker genes in TTX- and vehicle-treated neurons. Scale bar: scaled gene expression.

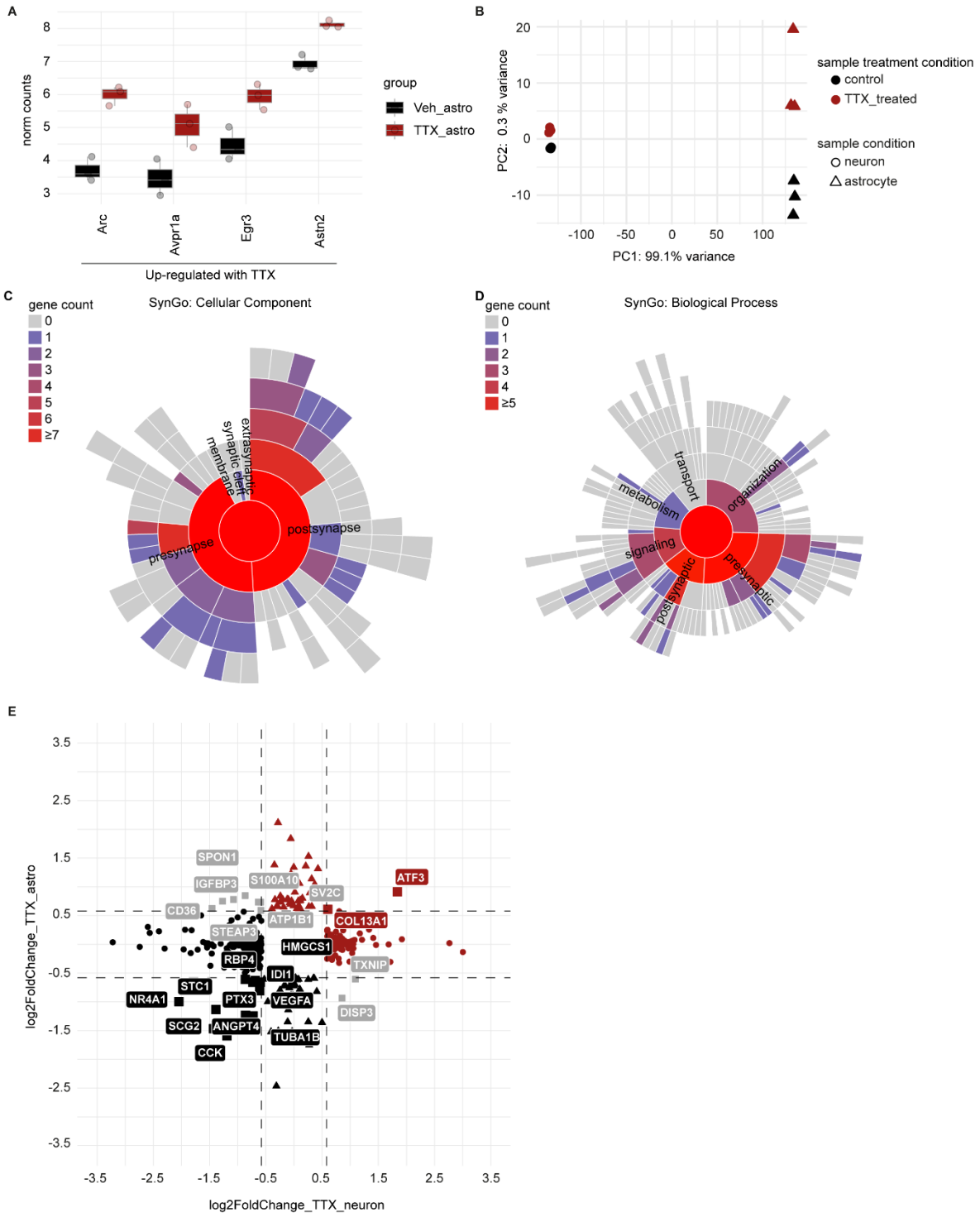

Supplemental Figure S5. Astrocytes and neurons share some transcriptional changes in response to TTX-induced neuronal activity suppression. Related to Figure 5. (A) Boxplot depicting the expression of selected DEGs (DESeq2 normalized counts), in both TTX- (red) and vehicle-exposed astrocytes (black). (B) Principal component analysis (PCA) of integrated RNA-sequencing counts from six samples of rat astrocytes and six samples of hiPSC-derived neurons. Shape of the points indicates the cell type (triangle = astrocyte, dot = neuron), and its colour depicts the received treatment (red = TTX and black = vehicle). (C-D) Sunburst plots for synaptic GO analysis of DEGs in response to TTX treatment in rat astrocytes co-cultured with hiPSC-derived neurons (Ctrl1, absolute $\log_2$ fold change (Log_2FC) > 0.58 and adjusted P value < 0.05), including Cellular Component (C) and Biological Process (D). 20 DEGs have a Cellular Component annotation, 14 DEGs for Biological Processes (a gene may have multiple annotations). 2 Cellular Component terms are significantly enriched at 1% FDR (testing

terms with at least three matching input genes), 0 for Biological Processes. Enrichment analyses were performed using 1-sided Fisher exact tests (with “greater than” for the alternative hypothesis) and the False Discovery Rate (FDR) method was applied for multiple testing correction. Synaptic GO analysis was performed with the SynGo (Koopmans *et al.*, 2019). Warmer colors represent the predominance of genes associated with the respective pathway. (E) Four-way volcano plot depicting expression changes per cell type in co-cultures of hiPSC-derived neurons and rat astrocytes treated with TTX (absolute Log2FC > 0.58 and adjusted p value < 0.05). Each data point represents a gene. Triangles depict DEGs only in astrocytes, circles indicate DEGs only in neurons, while squares depict DEGs in both astrocytes and neurons exposed to TTX. Color indicates the direction of change in gene expression activity in response to TTX treatment (red = up-regulated expression, black = down-regulated expression, gray = divergent direction in change in gene expression activity between the two cell types).

Supplemental discussion

Although not statistically over-represented, several genes differentially expressed by TTX-treatment have previously been associated with increased risk of neurodevelopmental disorders (NDDs) through genetic mutation, including *KCNN2* and *ZBTB20*. *KCNN2* encodes a voltage-independent potassium channel activated by intracellular calcium, and is thought to regulate neuronal excitability and synaptic transmission (Willis et al., 2017; Adelman et al., 2012; Ballesteros-Merino et al., 2012; Lin et al., 2008). The role of *KCNN2* in homeostatic plasticity, through dysregulation of neuronal excitability (Raghuram et al., 2017), may explain its link to NDDs. Similarly, *ZBTB20*, which encodes a zinc finger protein with an essential role in LTP and memory formation through modulation of NMDA receptor activity and activation of ERK and CREB (Ren et al., 2012), may be linked to NDDs also through its role in homeostatic plasticity. In astrocytes, the NDD-linked gene *Camk2a* (Kury et al., 2017) was differentially expressed after neuronal activity suppression with TTX. *Camk2a* encodes a calcium calmodulin-dependent protein kinase II Alpha (CaMKII; Silva et al., 1992). Inhibition of CaMKII signaling in cortical astrocytes reduces glutamate uptake and induces neurotoxic release of ATP (Ashpole et al., 2013). NDD-linked genetic mutations in *Camk2a* might act through an altered astrocytic contribution to homeostatic plasticity, as glutamate uptake plays a critical role in regulating the strength and the extent of receptor activation at excitatory synapses (Valtcheva and Venance, 2019). Taken together, our data highlights that mechanisms of neurodevelopmental disorders may involve homeostatic plasticity-related gene functions.

Supplemental tables (Table S1-3 were added as separate excel files)

Table S4. List of qPCR primers.

Gene name	Direction	Primer sequence (5' to 3')
h*BDNF*	forward	GGATGAGGACCAGAAAGT
h*BDNF*	reverse	AGCAGAAAGAGAAGAGGAG
h*NPTX1*	forward	CACCGAGGAGAGGGTCAAGAT
h*NPTX1*	reverse	CAGGGCGGTTGTCTTTCTGA
h*PPIA*	forward	CATGTTTTCCTTGTTCCCTCC
h*PPIA*	reverse	CAACACTCTTAACTCAAACGAGGA

Supplemental experimental procedures

HiPSC line origin and generation information

Ctrl1 originated from fibroblasts of a 30-year old and healthy male doner (Mandegar et al., 2016; Miyaoka et al., 2014), and reprogrammed using episomal vector-based reprogramming of the Yamanaka transcription factors Oct4, c-Myc, Sox2, and Klf4 (Takahashi and Yamanaka, 2006), and was tested for genetic integrity using SNP assay (Frega et al., 2019). Ctrl2 was derived from fibroblasts of a 36-year-old and healthy female doner (Kondo et al., 2017; Okita et al., 2011), and reprogrammed using episomal vector-based reprogramming of the Yamanaka factors, showing no karyotypical malformations (Frega et al., 2019). Ctrl3 was previously derived from a healthy 51-year old male doner and reprogrammed using expression of Yamanaka factors by non-integrating Sendai virus, was tested for genomic integrity based on SNP array (Frega et al., 2019).

Human iPSCs cell culture

HiPSCs were infected with Neurogenin-2 (Ngn2) and rtTA lentivirus. The vector utilized for generation of the rtTA lentivirus was pLVX-EF1α-(Tet-On-Advanced)-IRES-G418(R), which encodes a Tet-On advanced trans-activator under control of a constitutive EEF1A/EF1α promoter and has resistance to the antibiotic G418. The lentiviral vector for Ngn2 was pLVX-(TRE-tight)-(MOUSE)Ngn2-PGK-Puromycin(R), encoding Nng2 under control of a Tet-controlled promoter and the puromycin resistance gene under control of a constitutive PGK promoter. Both vectors were being transfected and packaged into lentiviral particles through using the packaging vectors psPAX2 lentiviral packaging vector (Addgene, 12260) and pMD2.G lentiviral packaging vector (Addgene, 12259). Medium was supplemented with puromycin (0.5 g/mL) and G418 (50 g/mL). Medium was refreshed every other day, and cells were passaged 1-2 times per week using an enzyme-free reagent (ReLeSR; Stem Cell Technologies, 05872). Cells were checked for mycoplasma contamination every two weeks. Droplet digital PCR (ddPCR) was performed to test genome integrity.

Neuronal differentiation

At DIV 1, the medium was changed to DMEM/F12 (Gibco, 11320074), which was supplemented with MEM non-essential amino acid solution NEAA (1:100, Sigma-Aldrich, M7145), N-2 Supplement (1:100, Gibco, 17502048), BDNF (10 ng/mL, PeproTech, 450-02), NT-3 (10 ng/mL, PeproTech, 450-03), doxycycline (4 µg/mL, Sigma, D9891), Primocin (0.1 mg/mL, Invivogen, ant-pm-2), and mouse laminin (0.2 mg/mL, Sigma-Aldrich, L2020). At DIV 2, freshly prepared rat astrocytes were added, in a 1:1 ratio, in order to support neuronal maturation. At DIV 3, the medium was fully changed to Neurobasal medium (Gibco, 21103049), which was supplemented with B-27 Supplement (1:50, Gibco, 17504044), GlutaMAX (1:100, Gibco, 35050038), Primocin (0.1 mg/mL, Invivogen, ant-pm-2), NT-3 (10 ng/mL, PeproTech, 450-03), BDNF (10 ng/mL, PeproTech, 450-02), and doxycycline (4 µg/mL). Cytosine β-D-arabinofuranoside (Ara-C, 2 µM, Sigma-Aldrich, C1768) was added once to remove proliferating cells from the cultures. From DIV 6 onwards, medium was 50% refreshed every other day. From DIV 10 onwards, the medium was additionally supplemented with 2.5% fetal bovine serum (FBS, Sigma, F2442) to support astrocyte viability. Neurons were differentiated to glutamatergic neurons by overexpression of Ngn2 until DIV 30 or DIV 49.

Procedure for TTX treatment and TTX withdrawal on MEA plates

At DIV 48, 50% pre-conditioned untreated culture medium was collected, and medium was then 50% refreshed. Specifically, 250 µL of the spent medium was collected in a 15 mL tube and stored at 4°C. Of the freshly prepared medium, 250 µL was added to cells. At DIV 49, a first MEA recording was performed by using the 24-well MEA system (Multichannel Systems, MCS GmbH, Reutlingen, Germany). After the MEA recording, 1 µM tetrodotoxin (TTX, Tocris, 1069) was added to certain wells. Five to ten min later, a MEA recording was performed again. The MEA plate was placed back to the incubator and incubated at 37°C, 5% CO2 for a specified number of hours (12, 24, 36, or 48 h). After that time, TTX was removed. Briefly, a first MEA recording was performed. All the spent medium was then aspirated. This washing step was repeated three times, in order to remove TTX completely. Then, 50% pre-conditioned untreated culture medium and 50% fresh medium were immediately added to the cells. At the last step, MEA recording was performed again. MEA plates were kept in the recording chamber for a longer measurement.

Immunocytochemistry

For the surface GluA2 staining and axon initial segment staining, neurons were fixed 48 h after TTX treatment at DIV 49. To ensure extracellular staining and prevent intracellular staining,

permeabilization was not performed when using anti-GluA2. The primary antibodies that were used are: Mouse anti-GluA1 (1:300, Sigma-Aldrich ABN241); Mouse anti-GluA2 (1:500, Invitrogen 32-0300); Mouse anti-Homer1 (1:300, Synaptic Systems 160 011); Rabbit anti-MAP2 (1:1000, Abcam, #ab32454); Guinea pig anti-Synapsin 1/2 (1:1000, Synaptic Systems 106004); Mouse anti-Ankyrin G (1:200, Invitrogen 33-8800). The secondary antibodies that were used are: Goat-anti-mouse Alexa 488 (1:1000, Invitrogen A11029); Goat anti-Rabbit Alexa Fluor 488 (1:1000, Invitrogen A11034); Goat anti-Guinea Pig Alexa Fluor 568 (1:1000, Invitrogen A11075); Goat anti-Mouse Alexa Fluor 568 (1:1000, Invitrogen A11031); Goat anti-Rabbit Alexa Fluor 647 (1:1000, Invitrogen A21245). Cells were imaged at 63x magnification using the Zeiss Axio Imager Z1 equipped with ApoTome. All conditions within a batch were acquired with the same settings in order to compare signal intensities between different experimental conditions. Fluorescent images were analysed using FIJI software. The number of GluA2 puncta was determined per individual cell via manual counting and divided by the dendritic length of the neuron. AIS start and end positions were obtained at the proximal and distal axonal positions.

Chemicals

TTX and 1-naphthyl acetyl spermine trihydrochloride (NASPM) were freshly prepared into concentrated stocks and stored frozen at −20°C. TTX was dissolved in distilled water (1 mM, Tocris 1069); NASPM was dissolved in distilled water (100 mM, Tocris 2766). For NASPM experiments on MEAs, immediately before adding NASPM to the cells, an aliquot of the concentrated stock was first diluted 1:100 at room temperature in Dulbecco's phosphate-buffered saline (DPBS) and vortexed briefly. Then, the appropriate amount of working dilution (1:100, the final concentration of NASPM was 1 µM) was added directly to wells on the MEA after cells were refreshed with 50% pre-conditioned untreated culture medium and 50% fresh medium, and mixing was primarily through diffusion into the cell culture medium.

MEA recordings and data analysis

Briefly, spontaneous electrophysiological activity of hiPSC-derived neurons grown on MEAs was recorded for 10 min. Before recording, MEA plates were in exploring status for 10 min, in order to adapt in the recording chamber. After 10 min, recording started. During the recording, the temperature was maintained constantly at 37°C, and the evaporation and pH changes of the medium were prevented by inflating a constant, slow flow of humidified gas (5% CO2 and 95% O2) onto the MEA plates (with the lid on). The signal was sampled at 10 kHz, filtered with a high-pass filter (i.e., Butterworth, 100 Hz cutoff frequency), and the noise threshold was set at ± 4.5 standard deviations.

Data analysis was performed off-line by using the Multi-well Analyzer (i.e., software from the 24-well MEA system that allows the extraction of the spike trains) and a custom-made MATLAB (The Mathworks, Natrick, MA, USA) code that allows the extraction of parameters describing the network activity. Mean firing rate (MFR) was defined as the average of the spike frequency of all 12 channels across one well of the MEA plate. For the burst detection, the number of bursting channels (above threshold 0.4 burst/s and at least 5 spikes in one burst with a minimal inter-burst-interval of 100 ms) was determined. A network burst was called when at least half of the channels in one well presented a synchronous burst.

Whole cell patch clamp

Whole cell patch clamp was performed as previously described (Mossink et al., 2022). Vehicle treated- or 48 h TTX-exposed coverslips were placed in the recording chamber, continuously perfused with oxygenated (95% O2/ 5% CO2) artificial cerebrospinal fluid (ACSF) at 32°C containing (in mM) 124 NaCl, 1.25 NaH2PO4, 3 KCl, 26 NaHCO3, 11 Glucose, 2 CaCl2, and 1 MgCl2. Patch pipettes with filament (ID 0.86 mm, OD1.05 mm, resistance 6-8 MΩ) were pulled from borosilicate glass (Science Products GmbH, Hofheim, Germany) using a Narishige PC-10 micropipette puller (Narishige, London, UK). For all recordings, a potassium-based intracellular solution containing (in mM) 130 K-Gluconate, 5 KCl, 10 HEPES, 2.5 MgCl2, 4 Na2-ATP, 0.4 Na3-ATP, 10 Na-phosphocreatine, and 0.6 EGTA was used, with a pH of 7.2 and osmolality of 290 mOsmol/L. Miniature postsynaptic currents (mEPSCs) were measured in ACSF containing 1 µM TTX. Cells were visualized with an Olympus BX51WI upright microscope (Olympus Life Science, PA, USA), equipped with a DAGE-MTI IR-1000E (DAGE-MTI, IN, USA) camera. A Digidata 1440A digitizer and a Multiclamp 700B amplifier (Molecular Devices) were used for data acquisition. Data was acquired at 10 KHz (mEPSCs), and a lowpass 1 kHz filter was used during recording. Recordings were not corrected for liquid junction potential (±10 mV), and they were discarded if series resistance reached >25 MΩ or dropped below a 10:0 ratio of Rm to Rs. mEPSCs were analysed using MiniAnalysis 6.0.2 (Synaptosoft Inc, GA, USA).

RNA-Sequencing
RNA from three biological replicates of vehicle-treated (Veh) and 48 h-TTX-treated (TTX) neurons (6 samples in total) were isolated using Quick-RNA Microprep kit (Zymo Research, R1051) according to the instructions of manufacturer. RNA quality was assessed using Agilent's Tapestation system (RNA High Sensitivity ScreenTape and Reagents, 5067–5579/80). RNA integrity number (RIN) values of all samples ranged between 8.3 and 8.7. Library preparation and paired-end RNA-sequencing were performed at CNAG-CRG, Centre for Genomic Regulation (CRG) (https://www.cnag.crg.eu/). Briefly, the RNA-Seq libraries were prepared with KAPA Stranded mRNA-Seq Illumina® Platforms Kit (Roche) starting from 500 ng of total RNA. The poly-A fraction enrichment was performed with oligo-dT magnetic beads, followed by the mRNA fragmentation. The strand specificity was achieved during the second strand synthesis performed in the presence of dUTP instead of dTTP. The blunt-ended double stranded cDNA was 3´adenylated, and Illumina platform-compatible adaptors with unique dual indexes and unique molecular identifiers (Integrated DNA Technologies) were ligated. The ligation product was enriched with 15 polymerase chain reaction (PCR) cycles. The libraries were sequenced on NovaSeq6000 (Illumina) in paired-end following the manufacturer's protocol for dual indexing. Image analysis, base calling, and quality scoring of the run were processed using the manufacturer's software Real Time Analysis, followed by generation of FASTQ sequence files.

RNA-Seq data processing
Raw count matrices were loaded in R v4.2.1. For Ensemble IDs that mapped to same gene symbols, we only considered the IDs with highest expression per sample. Then, count data were normalized using size factors method of DESeq2 (Love et al., 2014), and lowly expressed genes (< 15 normalized counts in three or more samples) were filtered. Principal component analysis was performed on variance-stabilized transformed counts, and differential expression analysis was performed with DESeq2 using lfcShrink and "apeglm" method (Love et al., 2014). Genes were considered differentially expressed if TTX-treatment induced a Log2FC > 0.58, with a false discovery rate (FDR)-adjusted P value < 0.05. Hierarchical clustering of the samples based on differentially expressed genes (DEGs) was performed with heatmap.2 function of gplots v3.1.3R package, using the Euclidean distance and "ward.D2" clustering method. Gene ontology (GO) enrichment analysis was performed on highly and lowly expressed genes after TTX-treatment independently, using the gost function of the R package gprofiler2 v0.2.1. Redundancy of enriched GO terms was accounted for with clustering analysis and aggregating terms with high semantic similarity, using the functions calculateSimMatrix and reduceSimMatrix with threshold=0.7 of the rrvgo v1.2.0 R package. We tested whether DEGs induced by TTX treatment were enriched for genes related to neurodevelopmental disorders (NDDs) and confident autism-related genes (Fu et al., 2022; Leblond et al., 2021), using one-tailed Fisher's exact test and adjusting P values with the FDR method. All plots were generated with custom code based on ggplot2 v.3.4.0 functions in R.

Gene expression analysis
Co-cultures of hiPSC-derived neurons and rat astrocytes were treated with or without 1 µM TTX (Tocris, 1069) at DIV 49 and harvested at DIV 51. RNA samples of vehicle- and TTX-treated conditions were isolated using Quick-RNA Microprep kit (Zymo Research, R1051) according to manufacturer's instructions.1 µg RNA was retro-transcribed into complementary strand of DNA (cDNA) by the iScript cDNA Synthesis Kit (Bio-Rad Laboratories, 1708891) according to the manufacturer's instructions. Quantitative real-time PCR (qRT-PCR) reactions were performed in QuantStudio Real-Time PCR systems by using GoTaq qPCR master mix 2x with SYBR Green (Promega, A6002) according to the manufacturer's protocol. We used human specific reference gene (*PPIA*) for our gene expression analyses. Used qRT-PCR primers were listed in Table S4. All samples were analyzed in triple in the same plate and placed in adjacent wells. Reverse transcriptase-negative controls and no template-controls were included in our procedures. The Ct value of every target gene was normalized against the Ct value of the reference genes [ΔCt = [Ct(target)-Ct(*PPIA*)]. The relative gene expression was calculated as $2^{-\Delta\Delta Ct}$ and used as fold change of gene expression when compared to corresponding control conditions [$2^{-\Delta\Delta Ct} = 2^{\Delta Ct(target)-\Delta Ct(control)}$].

Cross correlation
We implemented a Cross-Correlation (CC) script in Matlab using a common normalization factor (Eytan et al., 2004). Connectivity matrices were obtained by analysing the correlograms in a time window of 300 ms and using a 0.2 ms bin. In order to eliminate the contribution of spurious connections, a threshold (i.e., average of the weights of the total connections plus 2 times the value of the standard deviation) was applied. For each matrix the total number of links and their average weight have been calculated.

The total number of links: the number of functional connections within the nodes of the same network. The link weight: the average strength of the identified connections.

NBQX treatment procedure

In the experimental procedure involving the treatment of MEAs with NBQX (50 µM, Tocris #0373), prior to adding NBQX to the cells, the concentrated stock solution was diluted 1:10 in DPBS at room temperature and subjected to brief vortexing. Subsequently, certain volume of the resulting working dilution was directly added to the wells on the MEA, where the diffusion process facilitated its mixing into the 500 µL cell culture medium.

Supplemental references

Adelman, J.P., Maylie, J., and Sah, P. (2012). Small-conductance Ca2+-activated K+ channels: form and function. Annu Rev Physiol 74, 245-269. 10.1146/annurev-physiol-020911-153336.

Ashpole, N.M., Chawla, A.R., Martin, M.P., Brustovetsky, T., Brustovetsky, N., and Hudmon, A. (2013). Loss of calcium/calmodulin-dependent protein kinase II activity in cortical astrocytes decreases glutamate uptake and induces neurotoxic release of ATP. J Biol Chem 288, 14599-14611. 10.1074/jbc.M113.466235.

Ballesteros-Merino, C., Lin, M., Wu, W.W., Ferrandiz-Huertas, C., Cabanero, M.J., Watanabe, M., Fukazawa, Y., Shigemoto, R., Maylie, J., Adelman, J.P., and Lujan, R. (2012). Developmental profile of SK2 channel expression and function in CA1 neurons. Hippocampus 22, 1467-1480. 10.1002/hipo.20986.

Eytan, D., Minerbi, A., Ziv, N., and Marom, S. (2004). Dopamine-induced dispersion of correlations between action potentials in networks of cortical neurons. J Neurophysiol 92, 1817-1824. 10.1152/jn.00202.2004.

Frega, M., Linda, K., Keller, J.M., Gumus-Akay, G., Mossink, B., van Rhijn, J.R., Negwer, M., Klein Gunnewiek, T., Foreman, K., Kompier, N., et al. (2019). Neuronal network dysfunction in a model for Kleefstra syndrome mediated by enhanced NMDAR signaling. Nat Commun *10*, 4928. 10.1038/s41467-019-12947-3.

Kondo, T., Imamura, K., Funayama, M., Tsukita, K., Miyake, M., Ohta, A., Woltjen, K., Nakagawa, M., Asada, T., Arai, T., et al. (2017). iPSC-Based Compound Screening and In Vitro Trials Identify a Synergistic Anti-amyloid beta Combination for Alzheimer's Disease. Cell Rep *21*, 2304-2312. 10.1016/j.celrep.2017.10.109.

Koopmans, F., van Nierop, P., Andres-Alonso, M., Byrnes, A., Cijsouw, T., Coba, M.P., Cornelisse, L.N., Farrell, R.J., Goldschmidt, H.L., Howrigan, D.P., et al. (2019). SynGO: An Evidence-Based, Expert-Curated Knowledge Base for the Synapse. Neuron *103*, 217-234 e214. 10.1016/j.neuron.2019.05.002.

Kury, S., van Woerden, G.M., Besnard, T., Proietti Onori, M., Latypova, X., Towne, M.C., Cho, M.T., Prescott, T.E., Ploeg, M.A., Sanders, S., et al. (2017). De Novo Mutations in Protein Kinase Genes CAMK2A and CAMK2B Cause Intellectual Disability. Am J Hum Genet 101, 768-788. 10.1016/j.ajhg.2017.10.003.

Lin, M.T., Lujan, R., Watanabe, M., Adelman, J.P., and Maylie, J. (2008). SK2 channel plasticity contributes to LTP at Schaffer collateral-CA1 synapses. Nat Neurosci 11, 170-177. 10.1038/nn2041.

Love, M.I., Huber, W., and Anders, S. (2014). Moderated estimation of fold change and dispersion for RNA-seq data with DESeq2. Genome Biol 15, 550. 10.1186/s13059-014-0550-8.

Mandegar, M.A., Huebsch, N., Frolov, E.B., Shin, E., Truong, A., Olvera, M.P., Chan, A.H., Miyaoka, Y., Holmes, K., Spencer, C.I., et al. (2016). CRISPR Interference Efficiently Induces Specific and Reversible Gene Silencing in Human iPSCs. Cell Stem Cell *18*, 541-553. 10.1016/j.stem.2016.01.022.

Miyaoka, Y., Chan, A.H., Judge, L.M., Yoo, J., Huang, M., Nguyen, T.D., Lizarraga, P.P., So, P.L., and Conklin, B.R. (2014). Isolation of single-base genome-edited human iPS cells without antibiotic selection. Nat Methods *11*, 291-293. 10.1038/nmeth.2840.

Mossink, B., van Rhijn, J.R., Wang, S., Linda, K., Vitale, M.R., Zoller, J.E.M., van Hugte, E.J.H., Bak, J., Verboven, A.H.A., Selten, M., et al. (2022). Cadherin-13 is a critical regulator of GABAergic modulation in human stem-cell-derived neuronal networks. Mol Psychiatry 27, 1-18. 10.1038/s41380-021-01117-x.

Okita, K., Matsumura, Y., Sato, Y., Okada, A., Morizane, A., Okamoto, S., Hong, H., Nakagawa, M., Tanabe, K., Tezuka, K., et al. (2011). A more efficient method to generate integration-free human iPS cells. Nat Methods *8*, 409-412. 10.1038/nmeth.1591.

Raghuram, V., Weber, S., Raber, J., Chen, D.H., Bird, T.D., Maylie, J., and Adelman, J.P. (2017). Assessment of mutations in KCNN2 and ZNF135 to patient neurological symptoms. Neuroreport 28, 375-379. 10.1097/WNR.0000000000000754.

Silva, A.J., Paylor, R., Wehner, J.M., and Tonegawa, S. (1992). Impaired spatial learning in alpha-calcium-calmodulin kinase II mutant mice. Science 257, 206-211. 10.1126/science.1321493.

Takahashi, K., and Yamanaka, S. (2006). Induction of pluripotent stem cells from mouse embryonic and adult fibroblast cultures by defined factors. Cell *126*, 663-676. 10.1016/j.cell.2006.07.024.

Valtcheva, S., and Venance, L. (2019). Control of Long-Term Plasticity by Glutamate Transporters. Front Synaptic Neurosci 11, 10. 10.3389/fnsyn.2019.00010.

Willis, M., Trieb, M., Leitner, I., Wietzorrek, G., Marksteiner, J., and Knaus, H.G. (2017). Small-conductance calcium-activated potassium type 2 channels (SK2, KCa2.2) in human brain. Brain Struct Funct 222, 973-979. 10.1007/s00429-016-1258-1.